Human Molecular Genetics, 2006, Vol. 15, No. 6 **933–942**
doi:10.1093/hmg/ddl010
Advance Access published on February 1, 2006

MYC-containing double minutes in hematologic malignancies: evidence in favor of the episome model and exclusion of *MYC* as the target gene

Clelia Tiziana Storlazzi[1], Thoas Fioretos[2], Cecilia Surace[1], Angelo Lonoce[1], Angela Mastrorilli[1], Bodil Strömbeck[2], Pietro D'Addabbo[1], Francesco Iacovelli[1], Crescenzio Minervini[1], Anna Aventin[3], Nicole Dastugue[4], Christa Fonatsch[5], Anne Hagemeijer[6], Martine Jotterand[7], Dominique Mühlematter[8], Marina Lafage-Pochitaloff[8], Florence Nguyen-Khac[9], Claudia Schoch[10], Marilyn L. Slovak[11], Arabella Smith[12], Francesc Solè[13], Nadine Van Roy[14], Bertil Johansson[2] and Mariano Rocchi[1,*]

[1]Department of Genetics and Microbiology, University of Bari, Via Amendola 165/A, 70126 Bari, Italy, [2]Department of Clinical Genetics, University Hospital, Lund, Sweden, [3]Department of Hematology, Hospital Sant Pau, Barcelona, Spain, [4]Génétique des hemopathies, hopital Purpan, Toulouse, France, [5]Institut für Medizinische Biologie, Universitat Wien, Austria, [6]Center for Human Genetics, University of Leuven, Leuven, Belgium, [7]Unité de cytogénétique du cancer, CHUV, Lausanne, Switzerland, [8]Departement de Biopathologie, Institut Paoli-Calmettes, INSERM UMR 599, Université de la Méditerranée, Marseille, France, [9]Service d'Hematologie Biologique, Groupe Hospitalier Pitie-Salpetriere, Paris, France, [10]Kliniukum Grosshadern, LFL, München, Germany, [11]Division of Pathology, City of Hope National Medical Center, Duarte, CA, USA, [12]Department of Cytogenetics, Children's Hospital at Westmead, Westmead, Australia, [13]Laboratori de Citogenètica i Biologia Molecular, Servei de Patologia, Hospital del Mar, Barcelona, Spain and [14]Department of Medical Genetics, Ghent University Hospital, Ghent, Belgium

Received December 6, 2005; Revised January 19, 2006; Accepted January 27, 2006

Double minutes (dmin)—circular, extra-chromosomal amplifications of specific acentric DNA fragments—are relatively frequent in malignant disorders, particularly in solid tumors. In acute myeloid leukemia (AML) and myelodysplastic syndromes (MDS), dmin are observed in ~1% of the cases. Most of them consist of an amplified segment from chromosome band 8q24, always including the *MYC* gene. Besides this information, little is known about their internal structure. We have characterized in detail the genomic organization of 32 AML and two MDS cases with *MYC*-containing dmin. The minimally amplified region was shown to be 4.26 Mb in size, harboring five known genes, with the proximal and the distal amplicon breakpoints clustering in two regions of ~500 and 600 kb, respectively. Interestingly, in 23 (68%) of the studied cases, the amplified region was deleted in one of the chromosome 8 homologs at 8q24, suggesting excision of a DNA segment from the original chromosomal location according to the 'episome model'. In one case, sequencing of both the dmin and del(8q) junctions was achieved and provided definitive evidence in favor of the episome model for the formation of dmin. Expression status of the *TRIB1* and *MYC* genes, encompassed by the minimally amplified region, was assessed by northern blot analysis. The *TRIB1* gene was found over-expressed in only a subset of the AML/MDS cases, whereas *MYC*, contrary to expectations, was always silent. The present study, therefore, strongly suggests that *MYC* is not the target gene of the 8q24 amplifications.

*To whom correspondence should be addressed. Tel: +39 (0) 805443371; Fax: +39 (0) 805443386; Email: rocchi@biologia.uniba.it

INTRODUCTION

Double minutes (dmin)—the cytogenetic hallmark of extra-chromosomal genomic amplification—are small, paired, acentric chromatin bodies [(1) and references therein]. Different hypotheses have been proposed to explain how these circular structures, at times reaching several megabases in size, arise (2–4). In one model, the dmin, as well as the related homogeneously staining region (hsr) formation, is thought to be generated as a consequence of breakage-fusion-bridge cycles (5). An alternative proposed mechanism is the 'deletion-plus-episome' model (also known as 'episome model') (6–11), which postulates that DNA segments are excised from the chromosome, circularized and amplified by mutual recombination to produce dmin, or integrated into chromosomes to generate hsr. Data in support for this hypothesis have reported interstitial deletions of genes corresponding to the ones amplified in the dmin (12–16). Furthermore, episomes that gradually enlarge to dmin, with concomitant deletions, have been documented in Chinese hamster ovary cells (6) and in human neuroblastoma cell lines (17). In other instances, however, no deletions corresponding to the amplified chromosomal sequences were detected (18–21).

In order to clarify the mechanisms underlying the formation of dmin, we have performed a detailed genomic analysis of 34 acute myeloid leukemia (AML)/myelodysplastic syndrome (MDS) cases with *MYC*-containing dmin, using fluorescence *in situ* hybridization (FISH) and, when possible, quantitative polymerase chain reaction (PCR), junction sequencing and northern blot expression status of candidate genes in the amplified region. The results clearly supported the excision episome model for dmin genesis and strongly suggest that *MYC* is not the target gene of the amplification.

RESULTS

Clinical and cytogenetic features of the 34 AML/MDS cases are summarized in Supplementary Material, Table S1. FISH analysis with appropriate probes showed that dmin had large inter- and intra-individual size variation, and that the amplified *MYC* region was occasionally present both as extra-chromosomal dmin and intra-chromosomal hsr (Supplementary Material, Fig. S1). In 23 (68%) of 34 cases, the *MYC* probe did not hybridize to one of the chromosome 8 homologues (Supplementary Material, Table S1), indicating an accompanying submicroscopic deletion of the corresponding 8q24 segment; no deletions were observed in the remaining 11 (32%) cases (Supplementary Material, Figs S1 and S2). In two del(8q) cases (13 and 26), the deletion was observed in only a subpopulation of cells with *MYC*-containing dmin (12 and 96%, respectively), indicating the presence of two different clones with *MYC* amplification; these clones are referred to as 'a' (major clone) and 'b' (minor clone) (Supplementary Material, Fig. S1B). Additional chromosome 8 rearrangements further differentiating the 'deleted' and 'non-deleted' clones were identified in these two cases (Supplementary Material, Figs S1 and S2).

Sizes of the amplicons and interstitial deletions

In order to map precisely the proximal (PB) and distal (DB) breakpoints of the amplified genomic segments in the dmin, we utilized panels of bacterial artificial chromosome (BAC) clones (Fig. 1) selected according to the UCSC database (http://genome.ucsc.edu). In each dmin-positive case, reiterative FISH experiments were performed to identify BAC clones encompassing the breakpoints. These clones were identified if: (i) they consistently yielded fainter FISH signals on the dmin when compared with the signals on the normal chromosome(s) 8; (ii) the partially-overlapping proximal and distal clones yielded opposite results (negative or positive) on dmin; and (iii) these results were consistent with the position of PB or DB. The overall results are summarized in Figure 1 (examples in Supplementary Material, Fig. S2). The PBs mapped within an interval of ~500 kb (from 126 000 000 to 126 500 000) in 33 cases (97%) (Fig. 1A). In case 26, the two different clones with dmin [26a with del(8q) and 26b without del(8q)] displayed different PBs. The DBs were scattered within a ~3.7 Mb region (from 130 760 000 to 134 440 000), with most breakpoints (86%) within a 600 kb interval (from 130 760 000 to 131 360 000) (Fig. 1B). Cases 26, 30 and 32 harbored two subpopulations with different DBs. The amplicons in cases 29 and 32 were discontinuous, with both cases showing similar internal deletions, delineated by the clones RP11-976L13 and RP11-1146N6 (data not shown), a finding observed in only these two of 34 analyzed cases. By FISH mapping (Figs 1 and 2), the size of the amplicons varied from 4.29 Mb (case 8) to 7.83 Mb (case 9), with a commonly amplified segment of 4.26 Mb, harboring five known genes [from cen to tel: *TRIB1*, *NSE2*, *AF268618*, *MYC* and *AK093424* (Fig. 2)].

In 14 (61%) of 23 cases with 8q24 deletions (Supplementary Material, Table S1), the del(8q) corresponded with the amplified segments on the dmin by FISH studies (Fig. 2). This conclusion was based on the observation that: (i) the same BAC clone displayed a fainter signal on both the dmin and the del(8q) or on the derivative chromosomes in cases 13, 26 and 27 (Supplementary Material, Fig. S2A, SD–SF); and (ii) the flanking clones on both the dmin and the del(8q) showed consistent results. These data strongly indicate dmin formation by excision. In the remaining nine cases (39%), the deletions were larger than the corresponding amplified segment (Fig. 2 and Supplementary Material, Fig. S2B).

In 13 cases, real-time PCR experiments indicated 17- to 45-fold increases in *MYC* copy number (Supplementary Material, Fig. S3). Additional real-time PCR experiments, aimed at ascertaining the size of the amplified genomic segment (cases 2, 4, 8, 17, 18, 19, 23, 26 and 29), were in perfect agreement with the FISH results in all nine cases.

Cloning of the junction regions

Using forward and reverse primers designed on the distal and proximal amplicon borders and oriented towards the junction, the dmin junctions were successfully amplified in five cases (cases 2, 8, 18, 19 and 23) by long-range PCR experiments and nested PCR experiments were used to sequence the

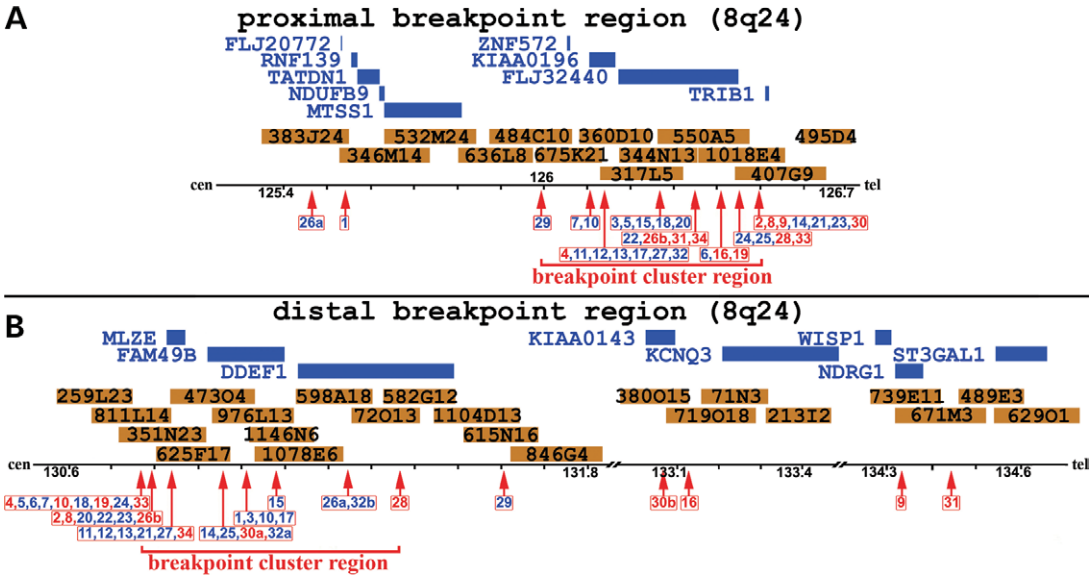

Figure 1. Distribution of the PB (**A**) and DB (**B**) of the amplicons and location of the PB (A) and DB (B) cluster regions in the 34 AML/MDS cases with *MYC*-containing dmin. Cases with or without accompanying 8q24 deletions (Supplementary Material, Table S1) are denoted in blue and red, respectively. Case 26 had two different cell populations—with (26a, blue) and without (26b, red) del(8)(q24q24)—with different PB and DB. The location of the BAC/PAC clones and the genes in the region are shown in brown and blue, respectively. Their positions were derived from the UCSC Genome Browser (http://genome.ucsc.edu/cgi-bin/hgGateway?DB = hg17; May 2004 release). In (B), cases 30 and 32 are shown twice because they had two different cell populations, with distinct DB, 'a' and 'b', respectively.

fusion regions (Fig. 3). These results clearly indicate a 'head-to-tail' arrangement of the amplicons. In addition, a single PCR product was obtained in all cases, suggesting, within the limits of agarose gel analysis, that the junction regions were not heterogeneous. Several attempts were made to clone the junction region of the deleted chromosome 8 in cases 18, 23, 26 and 29. Case 18 was the only case in which both dmin and deletion junctions were successfully amplified (Fig. 4). No PCR products were obtained in cases 4, 17, 26 and 29, although Southern blot analyses confirmed rearrangements of the intervals encompassing the DB identified by FISH and real-time PCR (data not shown) in cases 4 and 17. Vectorette PCR analyses, aimed at cloning the dmin junctions in cases 4, 17, 26 and 29, failed (data not shown).

Three of the 12 junctions (Fig. 3) were located within SINEs, including Alu (PB in case 2) and mammalian interspersed repeat (MIR) elements (PB and DB in case 23). The PB in both the del(8q) and the dmin in case 18 (Fig. 4) were mapped within a human self-chain alignment region (a region of the human genome where multiple DNA chains align). All other breakpoints were located within single copy sequences. Taken together, these results indicated that homologous recombination (HR) could have triggered a circularization event between two SINE (MIR) elements in only one case (case 23). Sequence analysis of the dmin junctions in cases 2 and 8 revealed a circularization event accompanied by an insertion of six and 19 nt, respectively; in addition, the insertion in case 8 contained a partial duplication of a 15 nt sequence flanking the breakpoint (Fig. 3). Non-homologous end-joining (NHEJ) microhomologies of two nt (CT) and four nt (ATTT) were detected at the amplicon junctions in cases 18 and 23. A two nt (AT) microhomology was also found at the deletion junction in case 18. Case 19 had an 'end-to-end' fusion between the proximal and the distal ends of the amplicon.

Interestingly, the PB and DB of the del(8)(q24q24) in case 18 were mapped 230 and 40 bp proximal to the PB and DB, respectively, of the amplicon (Fig. 4).

Bioinformatic analysis

GenAlyzer analysis did not reveal any extensive similar sequences in the chromosome 8 regions containing the PB and DB that could trigger a chromosome rearrangement resulting in dmin formation (data not shown). Consequently, we searched for other genomic properties of the target regions that might explain the clustering of the PB and DB. The results of the MAR-Wiz analyses are summarized in Supplementary Material, Fig. S4. The PB and DB cluster regions were located in two regions of low and infrequent matrix attachment region (MAR) potential. The proximal region contained three genes (*ZNF572*, *KIAA0196* and *FLJ324440*) within a 500 kb sequence and the distal region contained three genes (*MLZE*, *FAM49B* and *DDEF1*) within a 600 kb sequence, i.e. a gene density of one gene/167 kb and one gene/200 kb, respectively. The deleted/amplified region, on the other hand, contains only five known genes within a 4.3 Mb segment, i.e. a gene density of one gene/860 kb. Furthermore, the breakpoint cluster regions were shown to be poor in inter-genic, non-coding DNA, with the included genes being large and containing many exons, whereas the amplified region was found to be mainly non-coding, containing small genes with 1–3 exons. Thus, the PB and DB cluster regions are poor in MARs and rich in genes.

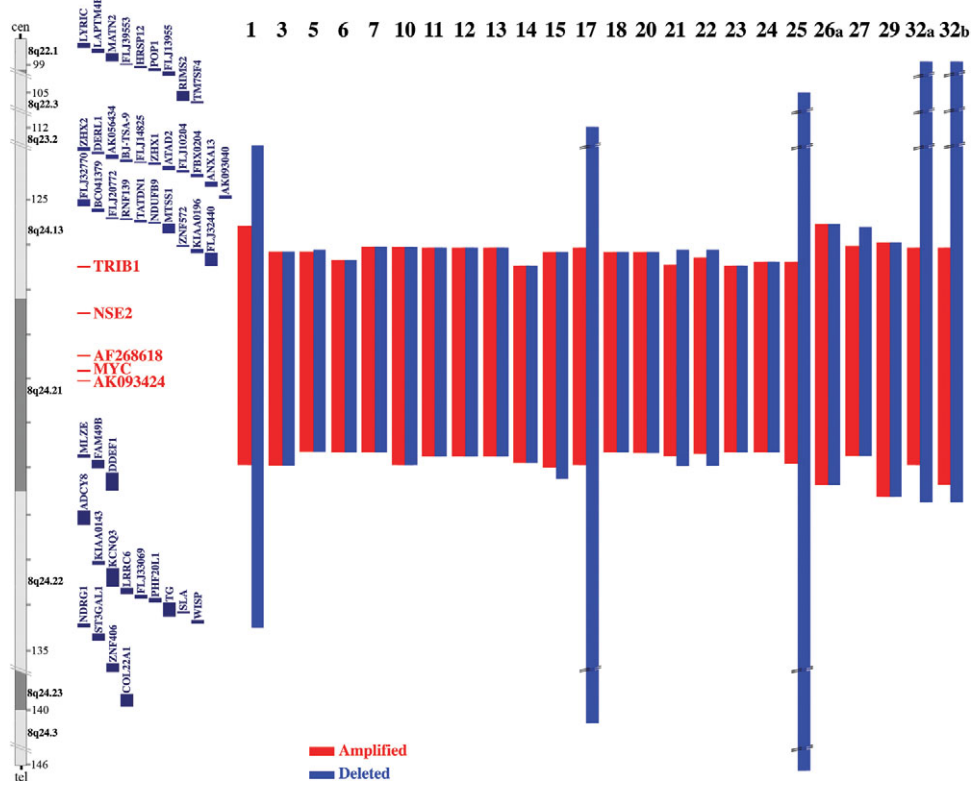

Figure 2. Sizes, as defined by FISH, of the amplifications (red) and deletions (blue) in the 23 cases with del(8)(q24q24). Case numbers (Supplementary Material, Table S1) are at the top of the figure. The five known genes within the commonly amplified segment are derived from the UCSC Genome Browser (May 2004 release; http://genome.ucsc.edu/cgi-bin/hgGateway?DB=hg17) and are denoted in red. Genes mapping outside, but in the vicinity of, the commonly amplified segment are denoted in blue.

Over-expression of *TRIB1* but not of *MYC*

Northern blot analyses of cases 6, 7, 8, 11, 12, 23, 27, 32 and 33 revealed over-expression of *TRIB1*, compared with AML and MDS cases without dmin or +8, in two of them (23 and 27), and a slight increase in case 6. Over-expression of *MYC* was not observed in any of these cases (Fig. 5). We have also searched for the presence of miRNAs in the amplified region, but no experimentally validated miRNAs were found (UCSC database http://genome.ucsc.edu).

DISCUSSION

In the present study, 34 AML/MDS cases with 8q24/*MYC* amplifications in the form of dmin (32 cases) or hsr (two cases) were analyzed in detail. Our results can be summarized as follows: (i) deletions corresponding to, or larger than, the amplicons were predominant (68%), suggesting post-replicative excision of circular DNA (episome) as the mechanism behind the dmin formation; (ii) the commonly amplified segment was 4.26 Mb in size and included four known genes in addition to *MYC*; (iii) even though the gene copy number of *MYC* was increased up to 45-fold, the gene was not over-expressed; (iv) the *TRIB1* gene was over-expressed in a subset of the cases; (v) the PB of the amplicons clustered within a 500 kb region in all but one case, whereas the DB clustered within a 600 kb region in 86% of cases; (vi) the circularization event of the amplicon appears consistent with error-prone NHEJ rather than mediated by HR; and (vii) the PB and DB cluster regions correspond to chromosomal segments with fewer MARs and more genes than the amplicons.

Expression studies

Detailed FISH mapping identified a commonly amplified 4.26 Mb genomic segment harboring five known genes [from cen to tel: *TRIB1*, *NSE2*, *AF268618*, *MYC* and *AK093424*; Fig. 2]. In a previous, two-case, investigation of *MYC*-containing dmin in AML/MDS, northern blot analyses showed no expression of *AK093424*, low expression of *MYC*, normal expression of *NSE2* and *AF268618*, with over-expression of *TRIB1*, suggesting that *TRIB1*, not *MYC*, was the most likely amplified target gene (22). The present study adds further support to the exclusion of *MYC* as the target gene, despite the fact that its copy number was increased 17- to 45-fold (Fig. 5 and Supplementary Material, Fig. S3) and further suggests that *TRIB1*, with over-expression in just two cases 23 and 27 (Fig. 5), may not be the critical gene either; however, a potential role for *MYC* at tumor initiation or early progression cannot be categorically excluded. Examples of discrepant gene copy number and expression levels have been reported in literature (23–25). Similarly, other undetected mutation(s), elsewhere in the genome, cannot be excluded as well. Regardless, dmins persistence, despite

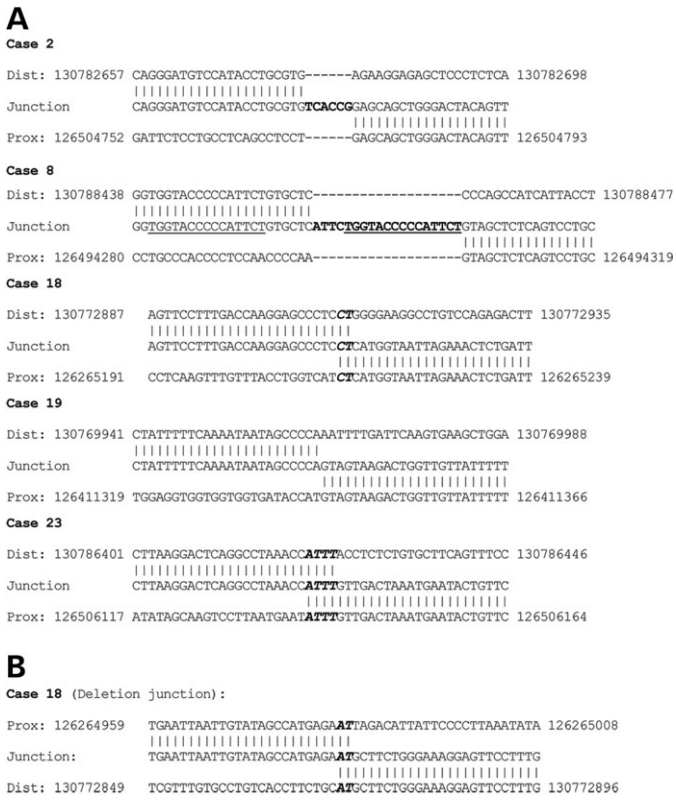

Figure 3. Sequences of the junctions of the amplicons in cases 2, 8, 18, 19 and 23 (**A**) and of the del(8)(q24q24) in case 18 (**B**). The junction sequences are aligned with the corresponding normal chromosome 8 sequences. Inserted nucleotides as well as microhomologies in the junctions are indicated in bold and in italics, respectively. Duplications of nucleotides within the dmin junction in case 8 are underlined. The numbers indicate the position at nucleotide level on the sequence of chromosome 8 according to the UCSC database, using the BLAT tool (http://genome.ucsc.edu/cgi-bin/hgBlat).

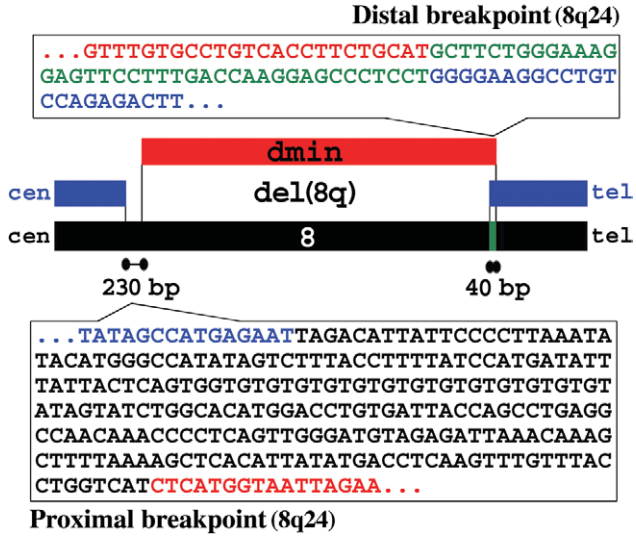

Figure 4. Schematic representation and sequences of the breakpoint regions of the del(8q) and of the amplicon in case 18. The red and blue nucleotides/bars indicate amplification and deletion borders, respectively. The 'black' nucleotides of the PB are deleted on the del(8q) but not amplified on the dmin, whereas the 'green' nucleotides of the DB are amplified on the dmin but not deleted on the del(8q).

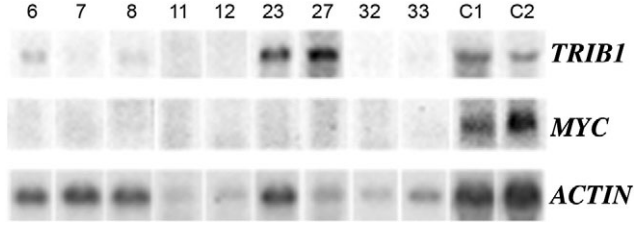

Figure 5. Northern blot analyses of *TRIB1* and *MYC* showing over-expression of *TRIB1* in cases 23 and 27, and a slight increase in case 6. In none of the cases was over-expression of *MYC* detected. β-Actin was used to verify successful transfer of the varying amounts (2–5 μg) of RNA available. C1 and C2 represent control RNA (10 μg) from one case of AML and MDS, respectively, without dmin or +8.

their intrinsic mitotic instability, strongly supports a proliferation advantage role for dmin.

Excision model

The majority (68%) of investigated cases harbored interstitial 8q24 deletions corresponding to the amplicons. Similar deletions have been reported in AML and MDS with *MYC*-containing dmin (12,22,26–30), *MLL* amplification (13), *NUP214/ABL1*-positive hematologic malignancies (15), *HMGA2/MDM2*- (14) and *MYC/ATBF1*-positive solid tumors (16). The latter authors have characterized in detail a complex translocation-excision-deletion-amplification in a neuroblastoma cell line, involving the *MYC* gene. The amplified 8q24 region (127 865 985 to 128 406 810 bp) was definitely smaller (541 kb) in comparison with the minimal interval we have reported (4.26 Mb). The deletion encompassed the region 127 865 985–130 479 097 bp (2.6 Mb).

A novel finding in the present study was the remarkable agreement, at the molecular cytogenetic level, of the deletions and amplicons. This observation and the integration of excised segments into various chromosomes (hsr formation), followed by intra-chromosomal amplification, as observed in cases 10 and 14, is most consistent with a mechanism of excision, circularization and subsequent amplification or the episome model (6,9). The finding that 11 (32%) cases did not show a concomitant del(8)(q24q24) does not oppose this conclusion: it may only indicate that the excision event was post-replicative. The circular element may segregate randomly with either normal or del(8q). Conversely, it is also possible that the deletions subsequently were 'corrected' as a result of somatic recombination between the two chromosome 8 homologues, a possibility consistent with the high frequency of partial uniparental disomies recently reported in AML (31,32). The present finding of two separate dmin-carrying populations—with and without del(8q)—in cases 13 and 26 would agree with both these possibilities.

Dmin breakpoint properties

Because the vast majority of PB and DB grouped together within two 'breakpoint cluster regions' (Fig. 1), a search of

fragile sites in these regions was undertaken. Two aphidicolin-inducible common fragile sites map within band 8q24. In fact, FRA8C (chr8:124,236,796–128,490,427) (33) spans the proximal region, whereas FRA8D (34) may span the distal region; this fragile site is known to start at chr8:129,026,266 (1.7 Mb proximal to the distal region) but its extension has, as yet, not been ascertained. Thus, common fragile sites may overlap with both breakpoint cluster regions identified in this study. However, size differences, i.e. 4 Mb of FRA8C versus 500 kb of the PB cluster region, and the elusive nature of aphidicolin-inducible fragile sites make it difficult to conclude that these fragile sites were involved in the genesis of the dmin. Considering that the dmin contained the *MYC*, the gene targeted by translocations in Burkitt lymphoma (BL), T-cell acute lymphocytic leukemia (T-ALL) and multiple myeloma (MM), it is tempting to speculate that the 8q24/*MYC* region is prone to chromosomal breakage and rearrangement. However, it should be stressed that the translocation breakpoints in BL and MM are located very close, within 1 Mb proximally and distally, to the *MYC* gene (34,35), whereas the PB and DB cluster regions in the dmin map 2 Mb proximally and distally to *MYC*.

Molecular cloning and sequencing of the amplicon junctions in five cases showed that the amplicon breakpoints were located in non-homologous genomic regions (Fig. 3); a finding not consistent with a circularization event triggered by HR pairing between repeated sequences. Only case 23 showed amplicon junctions within a SINE (MIR) element. In higher eukaryotes, NHEJ—an alternative
mechanism to error-free HR—has evolved to maintain genomic integrity after induction of DNA double-strand breaks (DSB) (36,37), which may occur after exposure to ionizing radiation and DNA topoisomerase II inhibitors, well-known agents associated with leukemogenesis (37,38). Conversely, error-prone NHEJ has been suggested to be involved in the generation of chromosome rearrangements, including deletions and translocations (39), and in many instances this repair process occurs at free ends showing either microhomologies of a few nucleotides or at ends displaying no homologies (40).

Vogt *et al*. (41) reported fusion of the amplicon ends mediated by microhomology-based NHEJ in six of seven dmin-carrying gliomas cases. In the present study, sequencing of the amplicon junctions showed nucleotide microhomologies in two of five cases (cases 18 and 23); the remaining three cases either displayed a blunt junction (19) or had insertions at the junctions (2 and 8) (Fig. 3). In case 8, 15/19 inserted nt corresponded to a partial duplication of the sequence flanking the DB, whereas the five nt segment inserted at the junction in case 2 was of unknown origin. Taken together, these results show that microhomology-based NHEJ is not the only mechanism involved in the fusing of the free ends of dmin. Furthermore, the failure to clone the junctions in cases 17, 19, 26 and 29 may indicate that the genomic architecture at the ends of the amplicons in these cases was even more complex, for example large insertions or heterogeneous amplicons sizes (cases 26 and 29), than in those that could be analyzed. In case 18, the junction on the del(8)(q24q24) was in agreement with the sequence junction of the amplicon, i.e. the PB and DB of the deletion-mapped 230 and 40 nt, respectively, centromeric to the PB and the DB of the amplicon. Thus, the amplified and deleted segment was identical except for a 230 nt proximal gap and a small 40 nt distal overlap (Fig. 4), the latter of which may be explained by the fill-in of the protruding single strand ends generated at DSB (42). In this case both the deletion and amplicon junctions were the result of a 2 nt microhomology-based NHEJ.

Because low copy repeat regions have been reported to play an important role in triggering inter- and intra-chromosomal HR in neoplasia-associated chromosomal abnormalities, such as t(9;22)(q34;q11.2) in chronic myeloid leukemia (CML) (43) and i(17)(q10) in AML, CML and MDS (44), a search for low copy chromosome 8 repeats surrounding the entire amplicon was performed (UCSC database, WSSD Duplication and Segmental Dups tracks). No intra-chromosomal duplicons were identified. However, the breakpoint cluster regions had fewer MARs but more genes than the amplicons (Supplementary Material, Fig. S4). Although these findings do not agree with previous results showing co-localization of MAR elements with the breakpoints in the AML-associated t(8;21)(q22;q22) (45), in the FRA16B AT-rich island (46), and in a topoisomerase II sensitive region in Chinese hamster (45–47), they are in accordance with the study by Hensel *et al*. (48) who reported *MLL* and *AFF1* (*AF4*) breakpoints in the ALL-associated t(4;11)(q21;q23) are usually located outside MARs.

The reason behind the fragility of the two identified breakpoint cluster regions could possibly be ascribed to the chromatin status of these regions. Transcribed DNA is less packed than inactive chromatin, and it is tempting to speculate that open chromatin is more vulnerable to DNA damage leading to chromosomal rearrangements (49–51). Considering that the breakpoint cluster regions harbored more genes than the amplicons, the former would be expected to have a higher transcription activity, less condensed chromatin structure and potentially more sensitive to DNA damage or enzymatic cleavage.

Concluding remarks

Although a complete understanding of the amplification processes underlying the dmin phenomenon remains a challenge, the current study provided the first sequence-based evidence supporting the episome model, and strongly suggests, contrary to expectations, that the *MYC* is not the target gene of dmin amplification.

MATERIALS AND METHODS

Patients

Thirty-four AML/MDS cases with *MYC*-containing dmin were collected from 14 different laboratories in Europe, US and Australia, comprising the largest series of dmin-positive AML and MDS cases reported to date. Basic clinical and cytogenetic features of the patients are listed in Supplementary Material, Table S1. The median age was 70 years (range 34 and 86 years) with 22 females and 12 males. All but two patients presented with AML, including 11 unclassified, five M1, 13 M2, one atypical M3, one M4 and one M5; the two

remaining cases were unclassified MDS and chronic myelomonocytic leukemia, respectively. In eight (24%) patients, dmin were found as the sole anomaly, eight (24%) additional cases displayed two karyotypic changes and the remaining 18 (53%) cases were cytogenetically complex.

Molecular cytogenetic analyses

MYC amplification was initially screened by FISH using the LSI C-MYC probe (Abbott, Rome, Italy), mapping to 8q24, or with the P1 artificial chromosome (PAC) clone RP1-80K22 (GenBank accession no. AF315312) covering the *MYC* gene. The *MYC*-containing dmin were then further characterized and mapped using contigs of BAC and PAC clones (Fig. 1), at 8q22-24, previously used to identify the breakpoint regions in 8q24-positive dmin (22). All clones belonged to the RP1 and RP11 libraries (http://www.chori.org/bacpac). Whole chromosome painting probes for chromosomes 3, 4 and 8 were derived from flow-sorted chromosomes (generously provided by Dr. Nigel Carter, Sanger Centre, Cambridge, UK) and amplified by degenerated oligonucleotide probe PCR. The α-satellite probe pZ8.4 (52) was used to identify the centromeric region of chromosome 8.

Co-hybridization experiments were performed by directly labeling the BAC/PAC clones with FITC-, Cy3- or Cy5-conjugated dUTP by nick-translation. Some of the probes were labeled with biotin–dATP and then detected with diethylaminocoumarin (DEAC)-conjugated streptavidin. FISH was performed as previously described (53). Digital images were obtained using a Leica DM-RXA2 epifluorescence microscope equipped with a cooled CCD camera (Princeton Instruments, Boston, MA). Cy3 (red), fluorescein (green), DEAC (blue), Cy5 (infra red) and DAPI (blue) fluorescence signals were detected using specific filters. Images were separately recorded as gray-scale images. Pseudocoloring and merging of images were performed using the Adobe Photoshop software. BAC clones that consistently yielded fainter FISH signals on the dmin, comp.

Multicolor-FISH

M-FISH, used to characterize the 8q24-amplification in the form of hsr in cases 10 and 29 (Supplementary Material, Fig. S1C), was performed in accordance with the manufacturer's instructions, using the commercially available 24-colour SpectraVysion probe (Abbott) (54). High-quality metaphase images were captured using a Leica DM-RXA2 epifluorescence microscope equipped with an eight-position automated filter wheel and a cooled CCD camera (Princeton Instruments). Six fluorescent images were captured per metaphase using filter combinations specific for SpectrumGold, SpectrumAqua, SpectrumGreen, FRed, Red and DAPI. Images were processed using the Leica CW4000 M-FISH software.

Amplicon analyses

Level of amplification. DNA was available in 13 of the 34 cases. The level of 8q24 (*MYC*) amplification in the 13 cases was determined by real-time PCR, with DNA from a healthy individual as a control. DNA was extracted from fresh or stored (−80°C) bone marrow samples according to standard methods. The DNA was amplified using the Applied Biosystems Real-Time PCR System 7300 using the SYBR Green PCR or the TaqMan PCR kits (Applied Biosystems, Monza, Italy). The PCR conditions were as follows: 2 min at 50°C, 10 min at 95°C, followed by 40 cycles of 15 s at 95°C and 1 min at 60°C for all the primer pairs and probes used. All measurements were performed at least in triplicate. Primers and probes were designed with the Primer Express® software v2.0 (Applied Biosystems). The primers were selected using the BLAT tool in the UCSC Human Genome Browser (55) (http://genome.ucsc.edu/cgi-bin/hgBlat); care was taken to avoid amplification of possible homologous sequences in other chromosomal locations (primer sequences available upon request). The level of *MYC* amplification in the dmin was calculated using the relative quantification approach based on the ΔΔCt method (56), which calculates the difference between the DNA quantity of the target gene and of the reference gene (*RNAseP*; Applied Biosystems) for each sample (ΔCt). This value was then compared with the human genomic control DNA (Applied Biosystems) which is used as a calibrator (ΔΔCt = ΔCt sample − ΔCt calibrator). The relative quantity (RQ) of DNA is determined as 2ΔΔCt, with the number of copies of the target gene in each sample tested being 2 × RQ.

Mapping of the dmin junctions at the sequence level. In nine cases (2, 4, 8, 17, 18, 19, 23, 26 and 29), sufficient amount of DNA was available for detailed characterization, at the sequence level, of the PB and DB, respectively of the amplicons. Multiple primer pairs that mapped at 10 kb intervals within the BAC clones spanning the breakpoints were designed and used to perform real-time PCR experiments, using DNA from a healthy individual as a control, in order to identify regions of switch between amplified and non-amplified sequences. The 10 kb segment encompassing the breakpoint was further narrowed down using the same approach, i.e. by selecting additional primer pairs within that region.

Junction sequencing. The information derived from the real-time PCR experiments described earlier, was utilized to design appropriate forward and reverse primers mapping in the DB and PB regions and used in long-range PCR experiments, with the aim of sequencing the dmin junction regions. Furthermore, in cases 18, 23, 26 and 29, the junctions in the del(8q) were investigated using long-range PCR with forward and reverse primers selected on the basis of the sequences flanking the amplicons on the dmin. In case of positive results, nested PCR experiments were performed. The long-range PCR analyses were performed using TaKaRa LA Taq™ (Cambrex Bio Science, Milan, Italy), and the nested PCR products containing the junction fragments were sequenced using the Big Dye Terminator Sequencing kits (Applied Biosystems). Reference genome sequence data were obtained from the UCSC browser (http://genome.ucsc.edu/cgi-bin/hgGateway?db=hg17; May 2004 release), and sequence comparison was performed using the BLAST software tool (www.ncbi.nlm.nih.gov/BLAST/).

Southern blot analyses. Southern blot analyses (57) were performed on cases 4 and 17 to validate the breakpoint results obtained by real-time PCR because the long-range PCR experiments, in these two cases, were unsuccessful (see Results). In brief, 2 μg of DNA from the patients and a healthy control were digested with *Bgl*II and *Eco*RI (case 4) or *Hae*III (case 17) (Roche, Milan, Italy), electrophoresed on 0.5% agarose gels, and transferred and fixed onto nylon membranes (Hybond-N, Amersham Pharmacia Biotech, Cleveland, OH) using standard protocols. The ^{32}P-labeled probes 22distA1 (265 bp) and 19dist2 (400 bp) for cases 4 and 17, respectively, were generated by PCR amplification using the primers 22distA1 and 19dist2 (primer sequences available upon request).

Vectorette PCR. Cloning of the dmin junctions was performed using the Vectorette PCR experiments, using the Universal Vectorette™ System (Sigma Genosys, Milan, Italy) to, were performed on cases 4, 17, 26 and 29, in which the long-range PCR analyses were unsuccessful (see Results). After digestion of 1 μg DNA with *Hin*dIII and *Eco*RI (Roche) and ligation with T4 DNA ligase (Sigma Genosys) of the corresponding Vectorette units to the digested ends of the DNA samples, Vectorette PCR was performed according the manufacturer's protocol (http://www.sigma-genosys.com).

Northern blot analysis

Total RNA from the patients' bone marrow and control cells was extracted using the Trizol reagent as described by the manufacturer (Invitrogen, Stockholm, Sweden). Sufficient amounts of good quality RNA, between 2 and 5 μg, were obtained in nine cases. Total RNA were electrophoresed in 1% formaldehyde/formamide gels, blotted as described (58), and subsequently hybridized with ^{32}P-labeled probes generated by PCR amplification (primer sequences available upon request) of the genes investigated. The identity of all probes was verified by sequencing, using the BigDye mix (Applied Biosystems, Warrington, UK). The signals were detected by phosphorimaging. β-Actin was used as a probe to verify equal loading and successful transfer of RNA. The expression patterns of *TRIB1* and *MYC* were analyzed. These genes were chosen because of previous evidence that *TRIB1*—and not *MYC*—may be the target of 8q24 amplifications in hematologic malignancies (22). The *NSE2*, *AF268618* and *AK093424*, which also map within the commonly amplified segment (see Results), were not analyzed because a previous study showed that these genes were not over-expressed in AML and MDS with *MYC*-containing dmin (22).

Bioinformatics and sequence analyses

The chromosome 8 sequences used for bioinformatic analyses were obtained from the UCSC Genome Browser website (http://genome.ucsc.edu/cgi-bin/hgGateway?db=hg17; May 2004 release).

Low copy repeat analysis. Segmental duplications occurring within an 8 Mb genomic segment (chr 8: 124 550 000–132 550 000), including the entire 8q24 amplicon, were searched for using GenAlyzer, a program of the REPuter family (http://www.genomes.de/) (59), on a sequence downloaded from the UCSC website (ftp://hgdownload.cse.ucsc.edu/).

MARs potential analysis. Putative MARs were mapped by the use of MAR-Wiz 1.5 (http://www.futuresoft.org/MAR-Wiz/), which predicts matrix association potential (MAP) using the following criteria: AT and CG-richness, sequence motifs for curved and kinked DNA, presence of topoisomerase II recognition sites, and replication origins. Unmasked sequence data were submitted in 500 kb segments. The default settings for generating MAPs were used, except the clipping parameter. The latter value was modified in order to obtain graphs where the MAPs ranged from 0 to 18. The graphical outputs of the MAPs were aligned to form a single graph in Adobe Photoshop CS 8.0. Each peak represents the MAP value of a 1 kb sequence window. According to the MAR-Wiz online instructions, all the normalized peaks having MAP values greater than 10.8 (threshold value representing 0.6 times of the maximum value of 18) should be considered as hypothetical MARs. High MAP values in three successive windows strongly suggest the occurrence of a MAR.

SUPPLEMENTARY MATERIAL

Supplementary Material is available at HMG Online.

ACKNOWLEDGEMENTS

This work was supported by AIRC (Associazione Italiana per la Ricerca sul Cancro), FIRC (Fondazione Italiana per la Ricerca sul Cancro), the European LeukemiaNet (Workpackage 11–Cytogenetics), the Swedish Cancer Society and CA32102. C. Surace is the recipient of a FIRC 3-year fellowship. We are grateful to Dr Cheryl Willman and Dr Richard Harvey for providing samples 6–9 for this study; Lisa Robson, Luke St. Heaps, Sara Diaz, for the FISH studies for cases 1, 5, 16; Dr Valérie Parlier and Dr Valérie Beyer for their contribution to the study of cases 11–13, 27, 34.

Conflict of Interest statement. None declared.

REFERENCES

1. Hahn, P.J. (1993) Molecular biology of double-minute chromosomes. *Bioessays*, **15**, 477–484.
2. Windle, B., Draper, B.W., Yin, Y.X., O'Gorman, S. and Wahl, G.M. (1991) A central role for chromosome breakage in gene amplification, deletion formation, and amplicon integration. *Genes Dev.*, **5**, 160–174.
3. Masuda, A. and Takahashi, T. (2002) Chromosome instability in human lung cancers: possible underlying mechanisms and potential consequences in the pathogenesis. *Oncogene*, **21**, 6884–6897.
4. Stark, G.R. and Wahl, G.M. (1984) Gene amplification. *Annu. Rev. Biochem.*, **53**, 447–491.
5. Mc Clintock, B. (1951) Chromosome organization and genic expression. *Cold Spring Harb. Symp. Quant. Biol.*, **16**, 13–47.
6. Carroll, S.M., DeRose, M.L., Gaudray, P., Moore, C.M., Needham-Vandevanter, D.R., Von Hoff, D.D. and Wahl, G.M. (1988) Double minute chromosomes can be produced from precursors derived from a chromosomal deletion. *Mol. Cell. Biol.*, **8**, 1525–1533.

7. Wahl, G.M. (1989) The importance of circular DNA in mammalian gene amplification. *Cancer Res.*, **49**, 1333–1340.
8. Stark, G.R., Debatisse, M., Giulotto, E. and Wahl, G.M. (1989) Recent progress in understanding mechanisms of mammalian DNA amplification. *Cell*, **57**, 901–908.
9. Savelyeva, L. and Schwab, M. (2001) Amplification of oncogenes revisited: from expression profiling to clinical application. *Cancer Lett.*, **167**, 115–123.
10. Von Hoff, D.D. (1991) New mechanisms of gene amplification in drug resistance (the episome model). *Cancer Treat. Res.*, **57**, 1–11.
11. Maurer, B.J., Lai, E., Hamkalo, B.A., Hood, L. and Attardi, G. (1987) Novel submicroscopic extrachromosomal elements containing amplified genes in human cells. *Nature*, **327**, 434–437.
12. Slovak, M.L., Ho, J.P., Pettenati, M.J., Khan, A., Douer, D., Lal, S. and Traweek, S.T. (1994) Localization of amplified *MYC* gene sequences to double minute chromosomes in acute myelogenous leukemia. *Genes Chromosomes Cancer*, **9**, 62–67.
13. Streubel, B., Valent, P., Jager, U., Edelhauser, M., Wandt, H., Wagner, T., Buchner, T., Lechner, K. and Fonatsch, C. (2000) Amplification of the *MLL* gene on double minutes, a homogeneously staining region, and ring chromosomes in five patients with acute myeloid leukemia or myelodysplastic syndrome. *Genes Chromosomes Cancer*, **27**, 380–386.
14. Roijer, E., Nordkvist, A., Strom, A.K., Ryd, W., Behrendt, M., Bullerdiek, J., Mark, J. and Stenman, G. (2002) Translocation, deletion/amplification, and expression of HMGIC and MDM2 in a carcinoma ex pleomorphic adenoma. *Am. J. Pathol.*, **160**, 433–440.
15. Graux, C., Cools, J., Melotte, C., Quentmeier, H., Ferrando, A., Levine, R., Vermeesch, J.R., Stul, M., Dutta, B., Boeckx, N. *et al.* (2004) Fusion of NUP214 to ABL1 on amplified episomes in T-cell acute lymphoblastic leukemia. *Nat. Genet.*, **36**, 1084–1089.
16. Van Roy, N., Vandesompele, J., Menten, B., Nilsson, H., De Smet, E., Rocchi, M., De Paepe, A., Pahlman, S. and Speleman, F. (2006) Translocation-excision-deletion-amplification mechanism leading to nonsyntenic coamplification of *MYC* and *ATBF1*. *Genes Chromosomes Cancer*, **45**, 107–117.
17. Hunt, J.D., Valentine, M. and Tereba, A. (1990) Excision of N-myc from chromosome 2 in human neuroblastoma cells containing amplified N-myc sequences. *Mol. Cell. Biol.*, **10**, 823–829.
18. Feo, S., Di Liegro, C., Mangano, R., Read, M. and Fried, M. (1996) The amplicons in HL60 cells contain novel cellular sequences linked to MYC locus DNA. *Oncogene*, **13**, 1521–1529.
19. Mangano, R., Piddini, E., Carramusa, L., Duhig, T., Feo, S. and Fried, M. (1998) Chimeric amplicons containing the *c-myc* gene in HL60 cells. *Oncogene*, **17**, 2771–2777.
20. Roelofs, H., Schuuring, E., Wiegant, J., Michalides, R. and Giphart-Gassler, M. (1993) Amplification of the 11q13 region in human carcinoma cell lines: a mechanistic view. *Genes Chromosomes Cancer*, **7**, 74–84.
21. Yoshida, H., Kondo, M., Ichihashi, T., Hashimoto, N., Inazawa, J., Ohno, R. and Naoe, T. (1998) A novel myeloid cell line, Marimo, derived from therapy-related acute myeloid leukemia during treatment of essential thrombocythemia: consistent chromosomal abnormalities and temporary *C-MYC* gene amplification. *Cancer Genet. Cytogenet.*, **100**, 21–24.
22. Storlazzi, C.T., Fioretos, T., Paulsson, K., Strombeck, B., Lassen, C., Ahlgren, T., Juliusson, G., Mitelman, F., Rocchi, M. and Johansson, B. (2004) Identification of a commonly amplified 4.3 Mb region with over-expression of C8FW, but not MYC in MYC-containing double minutes in myeloid malignancies. *Hum. Mol. Genet.*, **13**, 1479–1485.
23. Hyman, E., Kauraniemi, P., Hautaniemi, S., Wolf, M., Mousses, S., Rozenblum, E., Ringner, M., Sauter, G., Monni, O., Elkahloun, A. *et al.* (2002) Impact of DNA amplification on gene expression patterns in breast cancer. *Cancer Res.*, **62**, 6240–6245.
24. Pollack, J.R., Sorlie, T., Perou, C.M., Rees, C.A., Jeffrey, S.S., Lonning, P.E., Tibshirani, R., Botstein, D., Borresen-Dale, A.L. and Brown, P.O. (2002) Microarray analysis reveals a major direct role of DNA copy number alteration in the transcriptional program of human breast tumors. *Proc. Natl Acad. Sci. USA*, **99**, 12963–12968.
25. Heidenblad, M., Lindgren, D., Veltman, J.A., Jonson, T., Mahlamaki, E.H., Gorunova, L., van Kessel, A.G., Schoenmakers, E.F. and Hoglund, M. (2005) Microarray analyses reveal strong influence of DNA copy number alterations on the transcriptional patterns in pancreatic cancer: implications for the interpretation of genomic amplifications. *Oncogene*, **24**, 1794–1801.
26. Brunel, V., Sainty, D., Carbuccia, N., Arnoulet, C., Costello, R., Mozziconacci, M.J., Simonetti, J., Coignet, L., Gabert, J., Stoppa, A.M. *et al.* (1995) Unbalanced translocation t(5;17) in an typical acute promyelocytic leukemia. *Genes Chromosomes Cancer*, **14**, 307–312.
27. Reddy, K.S. and Sulcova, V. (1997) c-myc amplification in a preleukemia patient with trisomy 4 and double minutes: review of the unique coexistence of these two chromosome abnormalities in acute myelogenous leukemia. *Cancer Genet. Cytogenet.*, **95**, 206–209.
28. Thomas, L., Stamberg, J., Gojo, I., Ning, Y. and Rapoport, A.P. (2004) Double minute chromosomes in monoblastic (M5) and myeloblastic (M2) acute myeloid leukemia: two case reports and a review of literature. *Am. J. Hematol.*, **77**, 55–61.
29. Receveur, A., Ong, J., Merlin, L., Azgui, Z., Merle-Beral, H., Berger, R. and Nguyen-Khac, F. (2004) Trisomy 4 associated with double minute chromosomes and MYC amplification in acute myeloblastic leukemia. *Ann. Genet.*, **47**, 423–427.
30. Christacos, N.C., Sherman, L., Roy, A., DeAngelo, D.J. and Dal Cin, P. (2005) Is the cryptic interstitial deletion of 8q24 surrounding MYC a common mechanism in the formation of double minute chromosome? *Cancer Genet. Cytogenet.*, **161**, 90–92.
31. Raghavan, M., Lillington, D.M., Skoulakis, S., Debernardi, S., Chaplin, T., Foot, N.J., Lister, T.A. and Young, B.D. (2005) Genome-wide single nucleotide polymorphism analysis reveals frequent partial uniparental disomy due to somatic recombination in acute myeloid leukemias. *Cancer Res.*, **65**, 375–378.
32. Gorletta, T.A., Gasparini, P., D'Elios, M.M., Trubia, M., Pelicci, P.G. and Di Fiore, P.P. (2005) Frequent loss of heterozygosity without loss of genetic material in acute myeloid leukemia with a normal karyotype. *Genes Chromosomes Cancer*, **44**, 334–337.
33. Ferber, M.J., Thorland, E.C., Brink, A.A., Rapp, A.K., Phillips, L.A., McGovern, R., Gostout, B.S., Cheung, T.H., Chung, T.K., Fu, W.Y. *et al.* (2003) Preferential integration of human papillomavirus type 18 near the c-myc locus in cervical carcinoma. *Oncogene*, **22**, 7233–7242.
34. Ferber, M.J., Eilers, P., Schuuring, E., Fenton, J.A., Fleuren, G.J., Kenter, G., Szuhai, K., Smith, D.I., Raap, A.K. and Brink, A.A. (2004) Positioning of cervical carcinoma and Burkitt lymphoma translocation breakpoints with respect to the human papillomavirus integration cluster in FRA8C at 8q24.13. *Cancer Genet. Cytogenet.*, **154**, 1–9.
35. Fabris, S., Storlazzi, C.T., Baldini, L., Nobili, L., Lombardi, L., Maiolo, A.T., Rocchi, M. and Neri, A. (2003) Heterogeneous pattern of chromosomal breakpoints involving the MYC locus in multiple myeloma. *Genes Chromosomes Cancer*, **37**, 261–269.
36. Lieber, M.R., Ma, Y., Pannicke, U. and Schwarz, K. (2003) Mechanism and regulation of human non-homologous DNA end-joining. *Nat. Rev. Mol. Cell. Biol.*, **4**, 712–720.
37. Rassool, F.V. (2003) DNA double strand breaks (DSB) and non-homologous end joining (NHEJ) pathways in human leukemia. *Cancer Lett.*, **193**, 1–9.
38. Mistry, A.R., Felix, C.A., Whitmarsh, R.J., Mason, A., Reiter, A., Cassinat, B., Parry, A., Walz, C., Wiemels, J.L., Segal, M.R. *et al.* (2005) DNA topoisomerase II in therapy-related acute promyelocytic leukemia. *N. Engl. J. Med.*, **352**, 1529–1538.
39. Lengauer, C., Kinzler, K.W. and Vogelstein, B. (1998) Genetic instabilities in human cancers. *Nature*, **396**, 643–649.
40. Collis, S.J., DeWeese, T.L., Jeggo, P.A. and Parker, A.R. (2005) The life and death of DNA-PK. *Oncogene*, **24**, 949–961.
41. Vogt, N., Lefevre, S.H., Apiou, F., Dutrillaux, A.M., Cor, A., Leuraud, P., Poupon, M.F., Dutrillaux, B., Debatisse, M. and Malfoy, B. (2004) Molecular structure of double-minute chromosomes bearing amplified copies of the epidermal growth factor receptor gene in gliomas. *Proc. Natl Acad. Sci. USA*, **101**, 11368–11373.
42. Rebuzzini, P., Khoriauli, L., Azzalin, C.M., Magnani, E., Mondello, C. and Giulotto, E. (2005) New mammalian cellular systems to study mutations introduced at the break site by non-homologous end-joining. *DNA Repair (Amst)*, **4**, 546–555.
43. Saglio, G., Storlazzi, C.T., Giugliano, E., Surace, C., Anelli, L., Rege-Cambrin, G., Zagaria, A., Jimenez Velasco, A., Heiniger, A., Scaravaglio, P. *et al.* (2002) A 76-kb duplicon maps close to the *BCR* gene on chromosome 22 and the *ABL* gene on chromosome 9: possible

involvement in the genesis of the Philadelphia chromosome translocation. *Proc. Natl Acad. Sci. USA*, **99**, 9882–9887.
44. Barbouti, A., Stankiewicz, P., Nusbaum, C., Cuomo, C., Cook, A., Hoglund, M., Johansson, B., Hagemeijer, A., Park, S.S., Mitelman, F. *et al.* (2004) The breakpoint region of the most common isochromosome, i(17q), in human neoplasia is characterized by a complex genomic architecture with large, palindromic, low-copy repeats. *Am. J. Hum. Genet.*, **74**, 1–10.
45. Iarovaia, O.V., Shkumatov, P. and Razin, S.V. (2004) Breakpoint cluster regions of the *AML-1* and *ETO* genes contain MAR elements and are preferentially associated with the nuclear matrix in proliferating HEL cells. *J. Cell Sci.*, **117**, 4583–4590.
46. Jackson, J.A., Trevino, A.V., Herzig, M.C., Herman, T.S. and Woynarowski, J.M. (2003) Matrix attachment region (MAR) properties and abnormal expansion of AT island minisatellites in FRA16B fragile sites in leukemic CEM cells. *Nucleic Acids Res.*, **31**, 6354–6364.
47. Svetlova, E.Y., Razin, S.V. and Debatisse, M. (2001) Mammalian recombination hot spot in a DNA loop anchorage region: a model for the study of common fragile sites. *J. Cell Biochem.*, **81**, 170–178.
48. Hensel, J.P., Gillert, E., Fey, G.H. and Marschalek, R. (2001) Breakpoints of t(4;11) translocations in the human *MLL* and *AF4* genes in ALL patients are preferentially clustered outside of high-affinity matrix attachment regions. *J. Cell Biochem.*, **82**, 299–309.
49. Sbrana, I., Zavattari, P., Barale, R. and Musio, A. (1998) Common fragile sites on human chromosomes represent transcriptionally active regions: evidence from camptothecin. *Hum. Genet.*, **102**, 409–414.
50. Obe, G., Pfeiffer, P., Savage, J.R., Johannes, C., Goedecke, W., Jeppesen, P., Natarajan, A.T., Martinez-Lopez, W., Folle, G.A. and Drets, M.E. (2002) Chromosomal aberrations: formation, identification and distribution. *Mutat. Res.*, **504**, 17–36.
51. Surralles, J., Sebastian, S. and Natarajan, A.T. (1997) Chromosomes with high gene density are preferentially repaired in human cells. *Mutagenesis*, **12**, 437–442.
52. Archidiacono, N., Antonacci, R., Marzella, R., Finelli, P., Lonoce, A. and Rocchi, M. (1995) Comparative mapping of human alphoid sequences in great apes using fluorescence *in situ* hybridization. *Genomics*, **25**, 477–484.
53. Specchia, G., Albano, F., Anelli, L., Zagaria, A., Liso, A., Pannunzio, A., Archidiacono, N., Liso, V. and Rocchi, M. (2005) Molecular cytogenetic study of instability at 1q21 approximately q32 in adult acute lymphoblastic leukemia. *Cancer Genet. Cytogenet.*, **156**, 54–58.
54. Speicher, M.R., Gwyn Ballard, S. and Ward, D.C. (1996) Karyotyping human chromosomes by combinatorial multi-fluor FISH. *Nat. Genet.*, **12**, 368–375.
55. Kent, W.J. (2002) BLAT-the BLAST-like alignment tool. *Genome Res.*, **12**, 656–664.
56. Livak, K.J. and Schmittgen, T.D. (2001) Analysis of relative gene expression data using real-time quantitative PCR and the 2(-Delta Delta C(T)) method. *Methods*, **25**, 402–408.
57. Marsano, R.M., Milano, R., Minervini, C., Moschetti, R., Caggese, C., Barsanti, P. and Caizzi, R. (2003) Organization and possible origin of the Bari-1 cluster in the heterochromatic h39 region of *Drosophila melanogaster*. *Genetica*, **117**, 281–289.
58. Sambrook, J. and Russell, D. (2001) *Molecular cloning: A Laboratory Manual*. 3rd ed. Cold Spring Harbor Laboratory Press, Cold Spring Harbor, New York.
59. Choudhuri, J.V., Schleiermacher, C., Kurtz, S. and Giegerich, R. (2004) GenAlyzer: interactive visualization of sequence similarities between entire genomes. *Bioinformatics*, **20**, 1964–1965.